

AEGIS: CHANDRA OBSERVATION OF DEEP2 GALAXY GROUPS AND CLUSTERS

TAOTAO FANG^{1,2}, BRIAN F. GERKE³, DAVID S. DAVIS^{4,5}, JEFFREY A. NEWMAN^{6,7}, MARC DAVIS^{1,3}, KIRPAL NANDRA⁸, ELISE S. LAIRD⁹, DAVID C. KOO⁹, ALISON L. COIL^{7,10}, MICHAEL C. COOPER¹, DARREN J. CROTON¹, RENBIN YAN¹

(Received; Revised; Accepted)
Draft version July 18, 2018

ABSTRACT

We present a 200 *ksec* *Chandra* observation of seven spectroscopically selected, high redshift ($0.75 < z < 1.03$) galaxy groups and clusters discovered by the DEEP2 Galaxy Redshift Survey in the Extended Groth Strip (EGS). X-ray emission at the locations of these systems is consistent with background. The 3σ upper limits on the bolometric X-ray luminosities (L_X) of these systems put a strong constraint on the relation between L_X and the velocity dispersion of member galaxies σ_{gal} at $z \sim 1$; the DEEP2 systems have lower luminosity than would be predicted by the local relation. Our result is consistent with recent findings that at high redshift, optically selected clusters tend to be X-ray underluminous. A comparison with mock catalogs indicates that it is unlikely that this effect is entirely caused by a measurement bias between σ_{gal} and the dark matter velocity dispersion. Physically, the DEEP2 systems may still be in the process of forming and hence not fully virialized, or they may be deficient in hot gas compared to local systems. We find only one possibly extended source in this *Chandra* field, which happens to lie outside the DEEP2 coverage.

Subject headings: intergalactic medium – large-scale structure of universe – X-rays: galaxies: clusters – surveys – cosmology: observations

1. INTRODUCTION

Groups and clusters of galaxies are the most massive, dynamically relaxed objects in the universe. Past studies have focused on low to moderate redshifts (for reviews, see, e.g., Rosati et al. 2002; Voit 2005) due to the lack of reliable samples at high redshift. Recently, progress has been made in finding high- z clusters and groups, largely due to improved detection techniques and greater instrument sensitivities over large fields. For instance, the method of observing red sequence galaxies has proven to be efficient in identifying clusters with optical/near-IR imaging data (e.g., Gladders & Yee 2000). Also, *Chandra* and XMM-Newton have started to reveal X-ray clusters at redshift around unity (e.g., Rosati et al. 2002; Voit 2005). However, until now, no optically selected, spectroscopic sample has existed with sufficient size, sampling density, and redshift accuracy to identify large numbers of groups and clusters at $z > 0.5$.

The DEEP2 Galaxy Redshift Survey (Davis et al. 2003) has provided the first large spectroscopic galaxy catalog focused on $z \sim 1$, based on observations of

$\sim 5 \times 10^4$ galaxies. One of its four survey fields incorporates the Extended Groth Strip (EGS), which is the target of a multiwavelength survey called “All-wavelength Extended Groth Strip International Survey” (AEGIS; Davis et al. 2006). DEEP2 has produced the largest well-defined, spectroscopically selected sample of clusters and groups at high z yet (Gerke et al. 2005).

In this *Letter*, we investigate the X-ray properties of the DEEP2 groups and clusters which overlap an archival 200 *ksec* *Chandra* observation. The primary goal is to understand the relation between optical and X-ray properties of these systems at $z > 0.7$. At low z , simple scaling relations between X-ray quantities such as bolometric luminosity (L_X) and temperature (T_X) and optical quantities such as galaxy velocity dispersion (σ_{gal}) have been predicted and well studied (see, e.g., White et al. 1997; Allen & Fabian 1998; Markevitch 1998; Finoguenov et al. 2001; Ettori et al. 2002). However, high- z observations reveal a different trend: optically selected galaxy clusters tend to be less X-ray luminous than those with similar velocity dispersions at low redshifts (Castander et al. 1994; Bower et al. 1997; Holden et al. 1997; Lubin et al. 2002, 2004), while the X-ray selected samples tend to follow the local L_X - σ_{gal} relation (see, e.g., Ebeling et al. 2001; Valtchanov et al. 2004). The exact reason for the break-down of the L_X - σ_{gal} relation is still unclear. While previous studies of optical-X-ray relations have been limited only to a few large clusters, DEEP2 allows us to identify both clusters and groups at $z \sim 1$.

2. CHANDRA DATA ANALYSIS

The AO3 *Chandra* observation of the Groth-Westphal Strip (GWS), a subset of EGS, was taken on August 2002 (see Nandra et al. 2005 for observation details). This observation was taken using the imaging mode of the Advanced CCD Imaging Spectrometer (ACIS-I), which utilizes four CCD chips with a total field of view of

arXiv:astro-ph/0608382v1 17 Aug 2006

¹ Department of Astronomy, University of California, Berkeley, CA 94720

² Chandra fellow; fangt@astro.berkeley.edu

³ Department of Physics, University of California, Berkeley, CA 94720

⁴ Joint Center for Astrophysics, Department of Physics, University of Maryland, Baltimore County, 1000 Hilltop Circle, Baltimore, MD 21250, ddavis@milkyway.gsfc.nasa.gov

⁵ Laboratory for High Energy Astrophysics, Code 661, Greenbelt, MD 20771

⁶ Institute for Nuclear and Particle Astrophysics, Lawrence Berkeley National Laboratory, Berkeley, CA 94720

⁷ Hubble fellow

⁸ Astrophysics Group, Imperial College London, Blackett Lab., Prince Consort Road, London, SW7 2AW, UK

⁹ UCO/Lick Observatory, Department of Astronomy and Astrophysics, University of California, Santa Cruz, CA 95064

¹⁰ Steward Observatory, University of Arizona, Tucson, AZ 85721

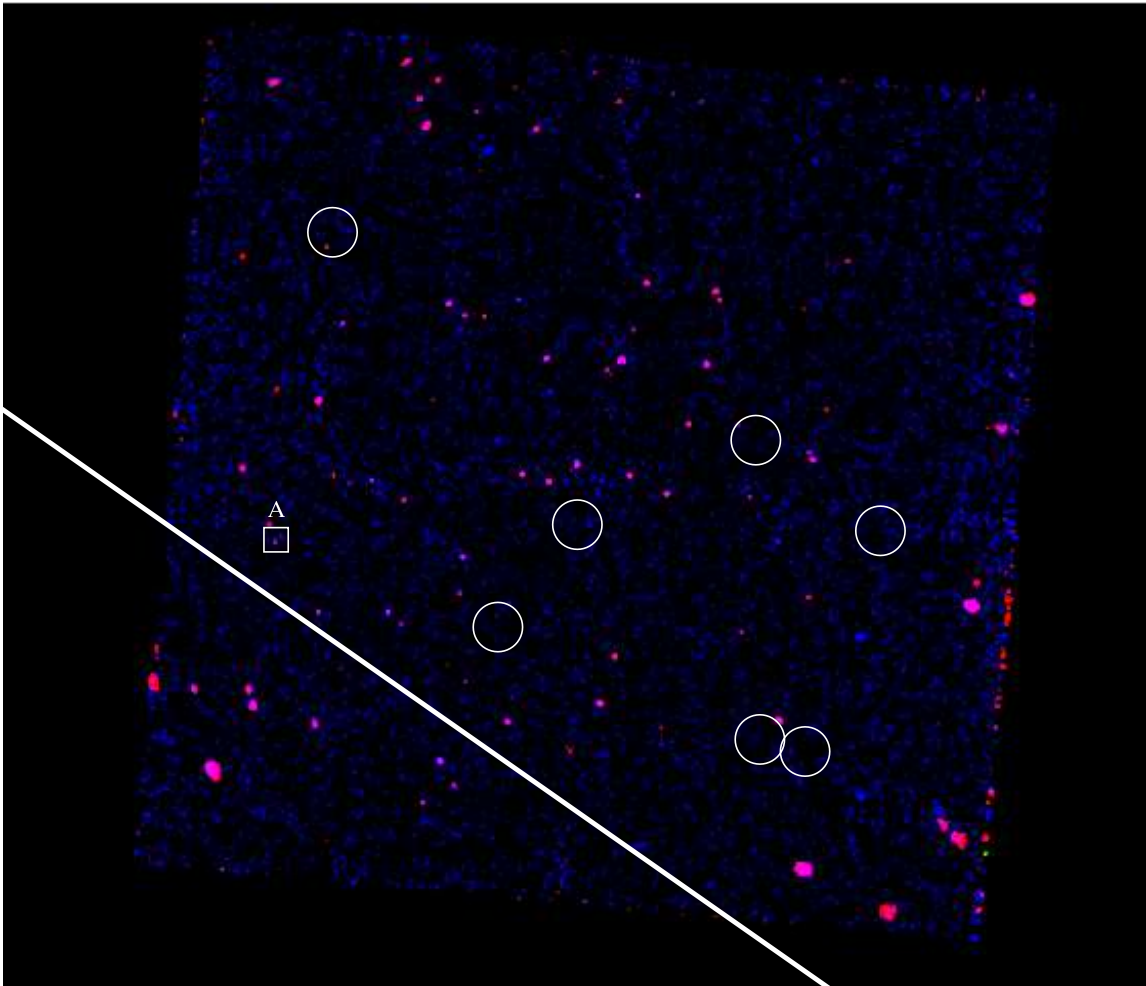


FIG. 1.— True-color image of the *Chandra* ACIS-I field, with north to the top and east to the left. The image is color-coded so that photons with energies at 0.54 – 2.05 keV, 2.05 – 3.50 keV, and 3.50 – 7.00 keV are in red, green, and blue, respectively. The DEEP2 survey covers the region to the north of the solid line. Circles represent DEEP2-identified systems. The white box labeled “A” indicates a possibly extended source.

$\sim 17' \times 17'$. A total of ~ 200 *ksec* exposure time was obtained over three separate observations, with IDs of #3305 (30 *ksec*), #4357 (85 *ksec*) and #4365 (85 *ksec*). Each observation was processed with the *Chandra* Interactive Analysis of Observations (CIAO) software package version 3.2¹¹. Specifically, we first identified and rejected hot pixel and afterglow events in the level 1 events file to create a new level 2 events file, using the CIAO tool “*acis_run_hotpix*”. We also removed bad pixels using observation-specific bad pixel files, selecting events with standard grades of 0, 2, 3, 4, 6, only, and cleaned the dataset of periods of anomalous background levels caused by strong background flares. The final level 2 events file was created by co-adding the three observations. Figure 1 shows a true-color image of the *Chandra* ACIS-I field after correction by exposure maps. The image is color-coded so that photons with energies at 0.54 – 2.05 keV, 2.05 – 3.50 keV, and 3.50 – 7.00 keV are shown as red, green, and blue, respectively.

We applied the Voronoi Tessellation and Percolation (VTP) algorithm (Ebeling & Wiedenmann 1993) to detection sources, using the *Chandra* tool “*vtpdetect*”.

While the VTP algorithm can be slow for large numbers of photons, it does have the advantage of finding faint, low surface-brightness features. We required that all detected sources should have at least 40 net photons, and set the maximum probability of being a false source to be 10^{-6} . We searched for potentially extended sources in three bands using VTP. This search algorithm yielded a total of 65 sources in the full band (0.5 – 7 keV), 45 in the soft band (0.5 – 2 keV), and 29 in the hard band (2 – 7 keV). The region corresponding to each detected source is represented by an ellipse with a semi-major axis of a and a semi-minor axis b .

To examine whether these sources are truly extended, we compared the size of the output ellipses with the size of instrument point spread function (PSF) at their corresponding off-axis angles. We computed the PSF using the MARX simulator¹². Specifically, single-energy photons at 1.5 keV were injected at different off-axis angles from the aim-point of ACIS-I, and then encircled energies at various percentage levels are calculated. We find that most sources have sizes from VPF smaller than the 95% encircled radius, indicating that they are indeed point

¹¹ See <http://asc.harvard.edu/ciao/>.

¹² See <http://space.mit.edu/ASC/MARX/>.

sources.

The only exception is source A at (RA, DEC)=(14:18:21.832, +52:26:5) (J2000), which is nearly twice as large as its predicted 95% radius and is designated by the white box in Figure 1. Visual inspection of this source in the exposure-corrected map shows that it indeed appears extended, although we cannot exclude the possibility that it is a mix of 2 – 3 faint point sources. The significance of the detection is $\sim 6\sigma$. Assuming the emission is from a weak extended source, we extracted the spectrum and fit it using the “APEC” thermal emission model with the software package XSPEC v12.0¹³. We fixed the neutral hydrogen absorption at the Galactic level, and assumed an abundance of 0.3 solar – the abundance that is typically found in the local galaxy groups and clusters. Due to the very limited number of net counts (~ 75 photons in the encircled region), we cannot constrain the temperature. Fixing it at 1 keV, we obtain a soft band absorbed flux (0.5 – 2 keV) of $\sim 1.54 \times 10^{-15}$ ergs cm^{-2} s^{-1} .

3. DEEP2 GROUP CATALOG

Details of the DEEP2 group sample and group finding methods can be found in Gerke et al. (2005). Here we briefly summarize information that is relevant to this *Letter*. Groups were identified using the Voronoi-Delaunay method (VDM, Marinoni et al. 2002). To insure a uniform group sample, we trimmed the DEEP2 sample in EGS to match the target selection rate and color cut used to select galaxies at $z > 0.7$ in the remaining DEEP2 fields. The group finding algorithm has been optimized using the mock catalogs presented in Yan et al. (2004).

We measure galaxy velocity dispersions in these groups using the “gapper” estimator (see, e.g., Beers et al. 1990). For the sample used in this paper, we require a minimum velocity dispersion of 300 km s^{-1} , above which the group velocity function is recovered well in mock catalogs (Gerke et al. 2005). This velocity dispersion cutoff roughly corresponds to a virialized halo mass of $\sim 10^{13} M_{\odot}$ at $z \sim 1$ with our adopted cosmology.¹⁴ We also require systems to have more than two member galaxies ($N_g > 2$). While in general errors on the measured velocity dispersion could be quite large for systems with small N_g (see discussion in § 5), we find that such errors are too large to have any constraining power at all when $N_g = 2$. With these cuts, we find a total of 7 groups and clusters in the DEEP2 data overlapping the *Chandra* pointing, with redshifts $0.75 < z < 1.03$. In Figure 1 we show the positions of the DEEP2 systems as white circles, with center indicating the mean position of member galaxies and radius $30''$. This radius roughly corresponds to a physical distance of ~ 250 kpc, a typical core radius for galaxy groups and clusters at high redshift.

4. RESULTS

4.1. High- z $L_X - \sigma_{gal}$ relation

None of the DEEP2 groups was detected directly by VPF. However, we can place upper limits on their X-ray

¹³ See <http://heasarc.gsfc.nasa.gov/docs/xanadu/xspec/>.

¹⁴ We adopt a standard Λ CDM cosmological model with a matter density of $\Omega_M = 0.3$ and a cosmological constant of $\Omega_{\Lambda} = 0.7$, and a Hubble constant of $H_0 = 100h \text{ km s}^{-1} \text{ Mpc}^{-1}$, where $h = 0.7$.

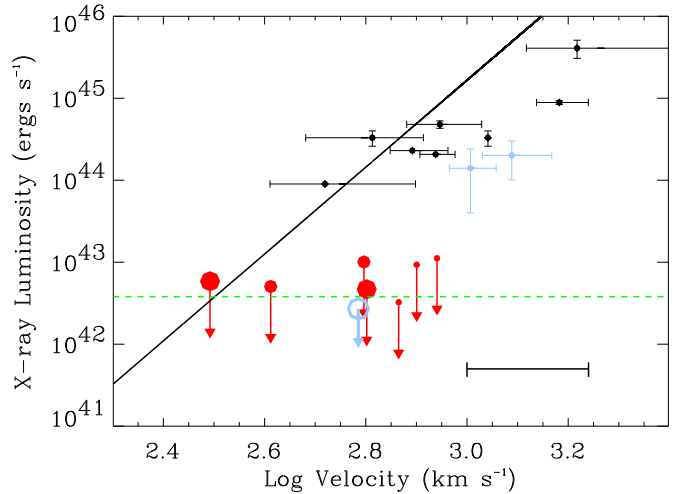


FIG. 2.— Bolometric X-ray luminosity vs. velocity dispersion. Filled red circles are 3σ upper limits on L_X for the DEEP2 systems, with their mean 1σ σ_{gal} uncertainty shown by the error bar at the bottom right. The size of each circle is proportional to the system richness, ranging from $N_g = 3$ to 6. The horizontal dashed green line indicates the 3σ upper limit from the stacked data. The solid dark line shows the local relation from Xue & Wu (2000). High- z ($z > 0.7$) X-ray selected clusters (black circles with error bars) are taken from Donahue et al. 1999; Gioia et al. 1999; Ebeling et al. 2001; Stanford et al. 2001; Valtchanov et al. 2004. Optically selected clusters are taken from Lubin et al. (2002) (blue circles with error bars) and Bauer et al. (2002) (open blue circle with arrow).

luminosity. Using Poisson statistics, we estimate the 3σ fluctuation in the X-ray background within a $30''$ radius aperture and take this as a 3σ upper limit on the X-ray photon counts from each system. Assuming thermal Bremsstrahlung radiation, we can then convert photon counts to flux using PIMMS¹⁵. To obtain flux, we also need a temperature estimate. Here we assume these systems follow the local, well-calibrated $\sigma - T_X$ relationship (see, e.g., Xue & Wu 2000). While as Lubin et al. (2004) reported, the high- z clusters are generally cooler, we found that for fixed photon counts, X-ray flux is not a very sensitive function of temperature: by lowering the temperature by a factor of 5, the flux varies by less than 20%. Knowing flux and redshift, we can then obtain the intrinsic X-ray luminosity of each galaxy group.

In Figure 2 we plot the bolometric X-ray luminosity as a function of velocity dispersion. The filled red circles are the 3σ upper limits on L_X for the DEEP2 systems. The size of the circles is proportional to N_g , i.e., the smallest circle corresponds to 3 members, and the largest corresponds to 6 members. We compute σ_{gal} errors by using Monte-Carlo realizations to obtain the distribution of true dispersions, given a richness and a dispersion measured with the “gapper” estimator; the mean uncertainty for the systems considered here is shown by the horizontal error bar at the bottom right of Figure 2.

The dark line in Figure 2 is the local $L_X - \sigma$ relation from Xue & Wu (2000). Since DEEP2 systems and cluster sample in Xue & Wu (2000) have similar σ_{gal} , we use their relation $L_X \propto \sigma^{5.30}$ that is appropriate for clusters of galaxies. Clearly, the DEEP2 systems are X-ray underluminous compared to the local $L_X - \sigma_{gal}$ relation,

¹⁵ Portable, Interactive Multi-Mission Simulator, see <http://cxc.harvard.edu/toolkit/pimms.jsp>

and this trend is more apparent for systems with larger velocity dispersions. This result is robust to changes in the adopted system radius. By increasing the radius to $30''$ to $40''$, the 3σ upper limit in L_X increases by $\sim 35\%$ only. We also have stacked *Chandra* images at their corresponding DEEP2 system positions to see whether we can find enhanced X-ray emission. The stacked image is consistent with background emission and provides a stronger constraint on the upper limit of L_X (shown by the dashed green line in Figure 2).

We overplot results from previous observations in Figure 2. X-ray selected clusters are plotted in black and optically selected clusters are plotted in blue. The open blue circle with an upper limit is taken from the ~ 1 Ms observation in the *Chandra* Deep Field north (Bauer et al. 2002), in which an optically identified cluster at $z \approx 0.85$ was not detected in X-ray. It is quite clear that at high- z , while optically selected clusters are X-ray underluminous, X-ray selected systems more or less follow the local $L_X - \sigma_{gal}$ relation.

4.2. Bias between galaxy and dark matter velocity dispersions

How well does the measured σ_{gal} reflect the dynamic state of high- z galaxy clusters and groups? A recent weak-lensing measurement of the optically selected cluster Cl 1604+4304 at $z = 0.9$ shows that galaxies are indeed good tracers of the dark matter, at least in this system (Margoniner et al. 2005). However, σ_{gal} measurements will tend to be higher than the velocity dispersion of the dark matter (σ_{DM}) due to an Eddington-like bias: low- σ_{DM} groups are much more common than high- σ_{DM} ones, so given the large velocity dispersion errors when N_g is small, it is more likely that a system above our velocity dispersion cutoff limit has a σ_{gal} which was scattered up from its true σ_{DM} value than one which was scattered down.

To test this, we have looked at systems in the DEEP2 mock catalogs (Yan et al. 2004) with $2 < N_g < 7$. In Figure 3, we plot the total mass within an overdensity of ~ 200 (M_{200} , top panel) and dark matter velocity dispersion (σ_{DM} , bottom panel) as a function of σ_{gal} . Clearly, a bias exists at high σ_{gal} end: for the same system σ_{gal} tends to be higher than σ_{DM} , and the system mass inferred from σ_{gal} is overestimated. Such bias typically is not seen at low redshift. At low z , simulations show that σ_{gal} in general follows σ_{DM} quite well, although some bias does exist at $\sim 10\%$ level for systems with less than 10 member galaxies (see, e.g., Davé et al. (2002)).

While this bias can partly explain why the DEEP2 systems are X-ray faint, it is unlikely that the non-detection of X-ray emission from all seven systems is caused by this effect. Based on the 3σ luminosity limit calculated in §2, non-detection would require that all seven systems have $\sigma_{DM} \lesssim 350$ km s $^{-1}$ if the local $L_X - \sigma_{gal}$ relation applies. We have performed a Monte-Carlo test by taking random sets of seven systems with measured velocity dispersions $300 < \sigma_{gal} < 1000$ km s $^{-1}$ in the mock catalog, and determine the chance that none of those systems have $\sigma_{DM} > 350$ km s $^{-1}$ is only 0.14%. So with $\sim 3\sigma$ confidence the DEEP2 systems must be X-ray underluminous.

5. DISCUSSION

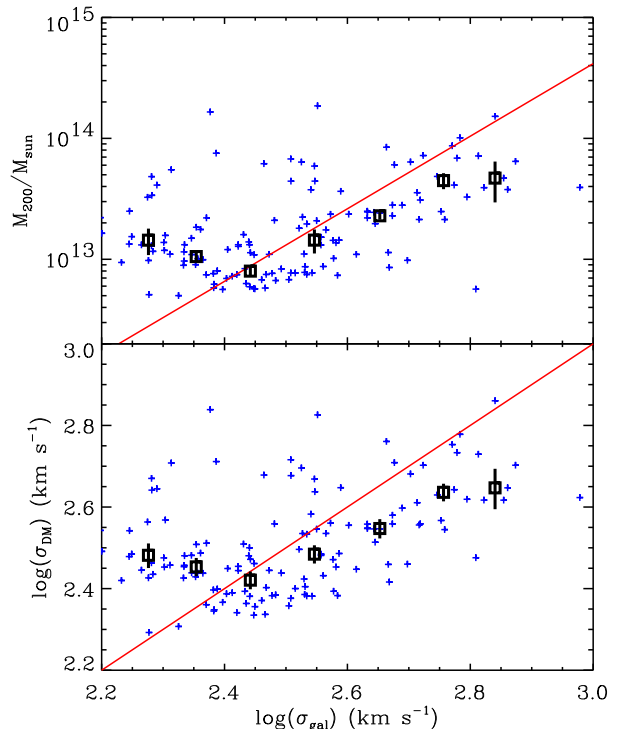


FIG. 3.— Halo mass (M_{200} , top panel) and dark matter velocity dispersion (σ_{DM} , bottom panel) as a function of galaxy velocity dispersion (σ_{gal}). The red lines in the top and bottom panels represent the theoretical prediction of M_{200} vs. σ_{gal} (Newman & Davis 2002), and $\sigma_{DM} = \sigma_{gal}$, respectively. Blue crosses are systems identified in the mock catalogs of Yan et al. (2004), and the open squares with error bars indicate the medians and standard error of M_{200} or σ_{DM} for equal-size bins in $\log(\sigma_{gal})$, with a bin size of 0.1.

In this *Letter*, we find evidence that spectroscopically selected galaxy groups and clusters at high redshift are X-ray underluminous; i.e., the upper limits of their X-ray luminosities are significantly below predictions from the local $L_X - \sigma_{gal}$ relation, unlike X-ray selected clusters at these redshifts. This confirms previous results showing that optically selected clusters at high z are weak X-ray sources.

While bias in the σ_{gal} measurement may contribute partly to the non-detection, it is unlikely to be the sole explanation. Physically, there are two basic reasons why spectroscopically selected systems at $z \sim 1$ might fall below the $L_X - \sigma_{gal}$ relation followed by X-ray selected clusters at these redshifts. The first is that the DEEP2 systems may be dynamically younger objects than those clusters which are easily detected in the X-ray. If the DEEP2 systems are not yet fully virialized, their gas may tend to be in cooler subclumps rather than at the temperature predicted from spherical-collapse models, and their galaxy velocity distribution may be multimodal rather than Gaussian, increasing the measured σ_{gal} (see, e.g., Frenk et al. 1996; Bower et al. 1997; Lubin et al. 2004).

An alternative is that these galaxy groups and clusters may be deficient in the hot gas that is necessary to produce detectable X-ray emission. DEEP2 systems do appear to be generally above the threshold mass beyond which cooling is predicted to be inefficient and a hot

atmosphere forms (Birnboim & Dekel 2003; Kereš et al. 2005; Croton et al. 2006). However, they may have passed that threshold only relatively recently in their history and may still be in the process of building a hot halo of substance. In this case L_X would be expected to remain low until a sufficient amount of hot gas had been accreted. We note that the average blue galaxy fraction is higher in DEEP2 groups than in local systems, reflecting the more common presence of the cold gas which feeds star formation (Gerke et al. 2006). al. 2006, in prep.)

Our *Chandra* observation is ~ 200 *ksec*. Two deeper (~ 1 *Msec*) exposures, the *Chandra* Deep Field South and North, yield a total of 18 (Giacconi et al. 2002) and 6 (Bauer et al. 2002) extended sources, respectively. Most of the sources are early type galaxies, poor groups and clusters. However, an early analysis on the *Chandra* Deep Field North with similar exposure did not detect any extended emission (Hornschemeier et al. 2001).

Our study highlights the importance of understanding groups and clusters of galaxies at high redshift. These systems present very different properties when compared with their counterparts at low redshift, indicating that complex processes govern the formation and evolution of large scale structures, which in turn have significant impact on galaxy evolution. We plan to investigate larger DEEP2 samples in the future to advance this work.

Acknowledgements: We thank Martin White, Joanne Cohn and Sandy Faber for useful discussions and comments. TF was supported by the NASA through *Chandra* Postdoctoral Fellowship Award Number PF3-40030 issued by the *Chandra* X-ray Observatory Center, which is operated by the Smithsonian Astrophysical Observatory for and on behalf of the NASA under contract NAS 8-39073. Also see Davis et al. (2006) in this volume for full acknowledgements.

REFERENCES

- Allen, S. W., & Fabian, A. C. 1998, MNRAS, 297, L57
 Bauer, F. E., et al. 2002, AJ, 123, 1163
 Beers, T. C., Flynn, K., & Gebhardt, K. 1990, AJ, 100, 32
 Birnboim, Y., & Dekel, A. 2003, MNRAS, 345, 349
 Bower, R. G., Castander, F. J., Ellis, R. S., Couch, W. J., & Boehringer, H. 1997, MNRAS, 291, 353
 Castander, F. J., Ellis, R. S., Frenk, C. S., Dressler, A., & Gunn, J. E. 1994, ApJ, 424, L79
 Croton, D. J., et al. 2006, MNRAS, 365, 11
 Davé, R., Katz, N., & Weinberg, D. H. 2002, ApJ, 579, 23
 Davis, M., et al. 2003, Proc. SPIE, 4834, 161
 Davis, M., et al. 2006, ApJL, submitted (this volume)
 Donahue, M., Voit, G. M., Scharf, C. A., Gioia, I. M., Mullis, C. R., Hughes, J. P., & Stocke, J. T. 1999, ApJ, 527, 525
 Ebeling, H., & Wiedenmann, G. 1993, Phys. Rev. E, 47, 704
 Ebeling, H., Jones, L. R., Fairley, B. W., Perlman, E., Scharf, C., & Horner, D. 2001, ApJ, 548, L23
 Ettori, S., De Grandi, S., & Molendi, S. 2002, A&A, 391, 841
 Finoguenov, A., Reiprich, T. H., Bohringer, H. 2001, A&A, 368, 749
 Frenk, C. S., Evrard, A. E., White, S. D. M., & Summers, F. J. 1996, ApJ, 472, 460
 Gerke, B. F., et al. 2005, ApJ, 625, 6
 Gerke, B. F., et al. 2006, ApJ, in preparation
 Giacconi, R., et al. 2002, ApJS, 139, 369
 Gioia, I. M., Henry, J. P., Mullis, C. R., Ebeling, H., & Wolter, A. 1999, AJ, 117, 2608
 Gladders, M. D., & Yee, H. K. C. 2000, AJ, 120, 2148
 Holden, B. P., Romer, A. K., Nichol, R. C., & Ulmer, M. P. 1997, AJ, 114, 1701
 Hornschemeier, A. E., et al. 2001, ApJ, 554, 742
 Kereš, D., Katz, N., Weinberg, D. H., & Davé, R. 2005, MNRAS, 363, 2
 Lubin, L. M., Mulchaey, J. S., & Postman, M. 2004, ApJ, 601, L9
 Lubin, L. M., Oke, J. B., & Postman, M. 2002, AJ, 124, 1905
 Margoniner, V. E., Lubin, L. M., Wittman, D. M., & Squires, G. K. 2005, AJ, 129, 20
 Markevitch, M. 1998, ApJ, 504, 27
 Marinoni, C., Davis, M., Newman, J. A., & Coil, A. L. 2002, ApJ, 580, 122
 Nandra, K., et al. 2005, MNRAS, 356, 568
 Newman, J. A., & Davis, M. 2002, ApJ, 564, 567
 Rosati, P., Borgani, S., & Norman, C. 2002, ARA&A, 40, 539
 Stanford, S. A., Holden, B., Rosati, P., Tozzi, P., Borgani, S., Eisenhardt, P. R., & Spinrad, H. 2001, ApJ, 552, 504
 Valtchanov, I., et al. 2004, A&A, 423, 75
 Voit, G. M. 2005, Rev. Mod. Phys., 77, 207
 White, D. A., Jones, C., & Forman, W. 1997, MNRAS, 292, 419
 Xue, Y.-J., & Wu, X.-P. 2000, ApJ, 538, 65
 Yan, R., White, M., & Coil, A. L. 2004, ApJ, 607, 739